

## Direct decay component of the giant-monopole-resonance region in $^{208}\text{Pb}$

W. Eyrich, K. Fuchs, A. Hofmann, U. Scheib, and H. Steuer

*Physikalisches Institut der Universität Erlangen-Nürnberg,  
D-8520 Erlangen, Federal Republic of Germany*

H. Rebel

*Kernforschungszentrum Karlsruhe, Institut für Angewandte Kernphysik,  
D-7500 Karlsruhe, Federal Republic of Germany*

(Received 24 January 1983)

The n decay of the giant-monopole-resonance region in  $^{208}\text{Pb}$  has been studied in an  $(\alpha, \alpha'n)$  coincidence experiment at  $E_\alpha = 104$  MeV. From the fast-neutron emission corresponding to the decay into the low lying single hole states in  $^{207}\text{Pb}$  a direct decay component of  $\approx 15\%$  was estimated for the resonant strength. In addition, evidence for a preequilibrium decay was found.

### I. INTRODUCTION

The decay properties of the giant resonances (GR's) are of special interest for the understanding of structure and dynamics of these collective modes of nuclear excitation. From a microscopical point of view, the GR's are built up by a coherent superposition of one-particle-one-hole (1p-1h) excitations. Having mostly excitation energies above particle emission thresholds, they usually decay by emission of neutrons, protons, and  $\alpha$  particles. The total decay width consists of an "escape width," which represents the "direct" decay owing to the coupling of the 1p-1h doorway state to the continuum, and a "spreading width," which reflects the coupling to more complicated  $np$ - $nh$  states. For the case of a dominating escape width, the decay leads predominantly to the low lying 1h states of the residual nucleus, whereas for a dominating spreading width all available states of the residual nucleus are populated following statistical rules. Besides these two extreme decay modes, which are generally used to classify the decay behavior (see, e.g., Ref. 1), intermediate "preequilibrium" modes should be possible as well.

A powerful tool to get detailed information about decay properties of isoscalar, electric GR's is the coincident observation of the decay particles after excitation through inelastic hadron scattering, especially of  $\alpha$  particles.

In the last few years, in light and medium nuclei, where a large fraction of the decay of the GR's takes place by emission of charged particles, a series of such experiments has been performed to study the  $E2$  GR.<sup>2,3</sup> They yielded a large direct decay component for the light nuclei, whereas with increasing mass the statistical decay becomes dominating.

In heavy nuclei the GR's predominantly decay by emission of neutrons because of the high Coulomb barriers for the emission of charged particles. Owing to the experimental difficulties connected with the spectroscopy of neutrons, especially in coincidence experiments, little experimental information about the neutron decay of the

isoscalar GR's is available. In a previous coincidence experiment<sup>4</sup> performed on  $^{208}\text{Pb}$  we observed the neutron decay of the region of the isoscalar electric GR's indirectly by  $(\alpha, \alpha'\gamma)$  measurements, where instead of the neutrons, the  $\gamma$  quanta of the subsequent decay in the residual nucleus  $^{207}\text{Pb}$  were observed in coincidence with the scattered  $\alpha$  particles. Moreover, we measured<sup>5</sup> the n decay of the region of the  $E2$  GR in  $^{208}\text{Pb}$  into the individual low lying states of  $^{207}\text{Pb}$  directly in an  $(\alpha, \alpha'n)$  coincidence experiment. The extracted branching ratios of the decay of the  $E2$  GR agree qualitatively with statistical model predictions. The angular correlation functions of the  $(\alpha, \alpha'\gamma)$  experiment, however, showed that the assumption of a pure statistical decay does not allow one to describe all decay data in a satisfactory way. In this work we report on the neutron decay of the  $E0$  GR region of  $^{208}\text{Pb}$  studied in an  $(\alpha, \alpha'n)$  coincidence experiment. In the following we first describe our experimental method, which is quite similar to that of Ref. 5, in some detail, and provide some supplementary remarks to our results of Ref. 5.

### II. EXPERIMENT

#### A. Beam handling

The measurements were performed with the energy analyzed 104 MeV  $\alpha$  particle beam at the Karlsruhe isochronous cyclotron with a resolution of about 100 keV. The experimental area was shielded against the analyzing magnet and the beam stop by thick walls of concrete, lead, and paraffin, leading to a strong background suppression. Moreover, a very careful beam preparation was absolutely necessary for the feasibility of the experiment. The position and the profile of the beam spot on the target and other critical elements were monitored periodically during the experiment by ZnS screens. A control even more sensitive than this optical observation proved to be the counting rates of the Ge(Li)  $\gamma$  detectors of the simultaneously performed  $(\alpha, \alpha'\gamma)$  coincidence experiment,<sup>5</sup> which yielded a sharp minimum at optimum focusing.

### B. Scattering chamber and detectors

Figure 1 shows a cross section of the scattering chamber. The target consists of a self-supporting enriched  $^{208}\text{Pb}$  foil ( $\geq 99\%$ ) with a thickness of  $10\text{ mg/cm}^2$ . The  $\alpha$  particles are measured by four Si(Li) detectors in a maximum ( $\phi_{\alpha,c.m.}=24^\circ$ ) and in a minimum ( $\phi_{\alpha,c.m.}=17^\circ$ ) of the  $(\alpha,\alpha')$  angular distribution of the  $E0(E2)$  strength in order to get information about the decay of the resonating strength and the underlying background separately. To allow the measurement of  $(\alpha,\alpha',\gamma)$  angular correlations (not further discussed here, cf. Ref. 5) and of  $(\alpha,\alpha'n)$  angular correlations simultaneously, the chamber has the form of a "key hole" with thin walls (2 mm) of aluminum in the directions of the n and  $\gamma$  detectors.

The decay neutrons are detected by two plastic scintillators with a volume of  $25 \times 25 \times 3\text{ cm}^3$ . The n detectors are shielded against neutron and  $\gamma$  background radiation by lead, cadmium, and paraffin enriched with boron as shown in Fig. 2. A comparison of the counting rates with and without target showed that owing to this shielding system only less than 20% of the detected events came from background radiation. This ratio was measured to increase by more than a factor of 10 without shielding. We measured at the eight positions  $(\theta_n, \phi_n) = (101^\circ, \pm 112.5^\circ)$ ,  $(101^\circ, \pm 157.5^\circ)$ ,  $(143^\circ, \pm 112.5^\circ)$ , and  $(143^\circ, \pm 157.5^\circ)$ . The reason for the choice of these special angles [the z axis perpendicular to the  $(\alpha,\alpha')$  reaction plane, the x axis in the beam direction] will be given later.

The energy threshold of the n detectors was about 1 MeV; the lowest energy evaluated in the experiment was 1.3 MeV. The efficiency of the n detectors, which was measured by the use of monoenergetic neutrons from the reaction  $^{11}\text{B}(p,n)$  at the Erlangen tandem accelerator, turned out to be constant within about 10% in the energy region of interest, as can be seen from Fig. 3. As already mentioned in Ref. 5, we applied the time-of-flight technique to get sufficient energy resolution for the decay neutrons. The flight path was 1.5 m. The time of flight was measured with respect to the high frequency of the cyclotron. Using phase space cuts in the inner region of the cyclotron, a pulse width of  $\leq 0.6\text{ ns}$  (FWHM) was achieved. To drop out ambiguities between neutrons from successive

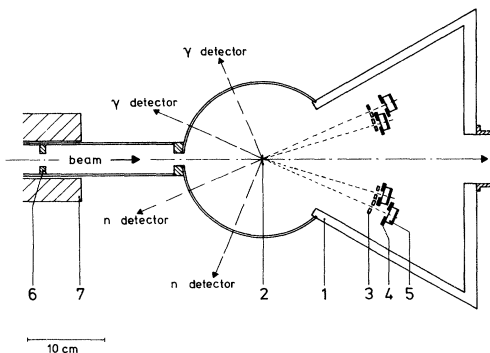


FIG. 1. Cross section of the scattering chamber and the detector arrangement: (1) scattering chamber; (2) target; (3) slits; (4) cooling plates; (5) Si(Li) detectors; (6) entrance slit; (7) lead shielding.

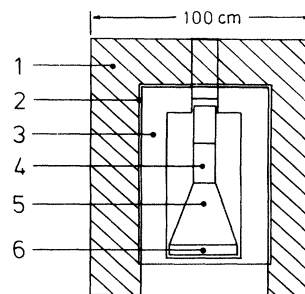


FIG. 2. Cross section of a neutron detector with shielding: (1) paraffin; (2) cadmium; (3) lead; (4) photomultiplier; (5) plastic lightguide; (6) scintillator.

cyclotron pulses, the standard pulse distance of 30 ns was stretched to 90 ns by an internal deflection system. Thus, for the parameters used, prompt  $\gamma$  quanta from the target appear clearly outside the region of the investigated neutrons. Therefore, n- $\gamma$  discrimination was unnecessary for this experiment.

The time resolution of the n detectors against the high frequency of the cyclotron was about 1.4 ns. This value was determined with monoenergetic neutrons obtained from a pulsed beam with a pulse width  $\leq 1.0\text{ ns}$  (FWHM) at the Erlangen tandem accelerator. It corresponds to an energy resolution between about 40 keV for the lowest evaluated energy ( $E_n = 1.3\text{ MeV}$ ) and about 400 keV for the fastest neutrons ( $E_n \approx 7\text{ MeV}$ ) from the region of the  $E0\text{ GR}$ . Thus, together with the energy resolution of the  $\alpha$  detectors of  $\approx 220\text{ keV}$ , an overall resolution of between about 250 and 500 keV was obtained in the coincident neutron spectra.

### C. Electronics and data evaluation

The setup of the electronics, which is displayed schematically in the block diagram of Fig. 4, was based on a fast-slow circuit technique. For simplicity, only one of the four  $\alpha$  detectors, one of the two n detectors, and one of the two  $\gamma$  detectors are shown. The outputs of the charge sensitive preamplifiers (PA) are split into energy and time branches. To get optimum time information, constant fraction triggering (CFT) was used in all branches. The signals of the neutron detectors were received by fast photomultipliers and bases. To get a well-defined threshold, the time-of-flight spectrum of the n

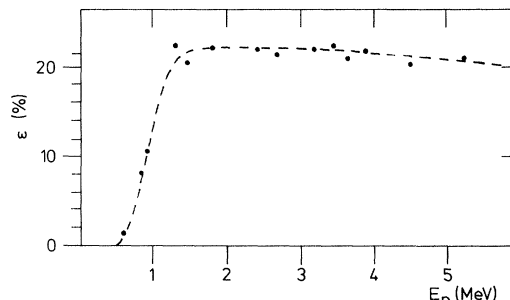


FIG. 3. Experimental efficiency as a function of energy for one of the used n detectors deduced from the  $^{11}\text{B}(p,n)$  reaction.

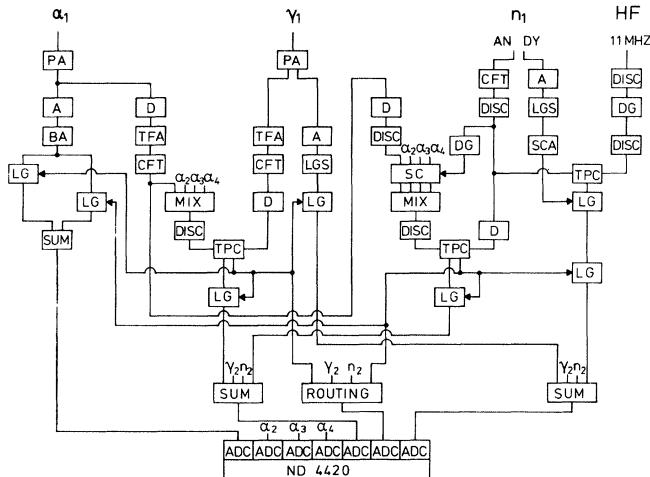


FIG. 4. Block diagram of the electronics (simplified): PA—preamplifiers; TFA—timing filter amplifiers; CFT—constant fraction triggers; D—delay lines; Disc—threshold discriminators; TPC—time-to-pulse-height converters; SC—strobed coincidence; SCA—single-channel analyzers; DG—delay and gate; A—amplifiers; LGS—stretchers; BA—biased amplifiers; LG—linear gates; Mix—mixers; SUM—sum amplifiers; ADC—analogue-to-digital converters.

detectors was gated by the dynode signals of the bases. In the  $\alpha$ -n circuit two coincidence units were used, one fast overlap coincidence (SC), and in a second step a time-to-pulse height converter (TPC). Thus, the overall dead time of the electronics could be reduced to less than 20% at counting rates of 50 kHz. The events recorded in list mode on magnetic tapes were defined to consist of the energy of the scattered  $\alpha$  particles, the time of flight of the neutrons or the energy of the  $\gamma$  quanta (not discussed here), and the time-of-flight difference (coincidence spectrum) between  $\alpha$  particles and neutrons or between  $\alpha$  particles and  $\gamma$  quanta. To control the electronics and to be able to correct for the dead time accurately, pulser signals were fed into the preamplifiers and photomultiplier bases simultaneously during all experimental runs.

#### D. Analysis and discussion

In the first step we measured and analyzed  $(\alpha, \alpha')$  singles scattering spectra in the angular region between about  $15^\circ$  and  $30^\circ$  in order to fix the angles of the  $(\alpha, \alpha'n)$  coincidence experiment. A simultaneous measurement at a maximum and a minimum of the  $E0$  angular distribution required a minimum angular distance of the  $\alpha$  detectors of about  $7^\circ$ , given by their size and the used scattering chamber. In Fig. 5 the singles  $\alpha$ -scattering spectra for the maximum (upper part of the figure) and the minimum (lower part of the figure) position at  $\phi_{\alpha, \text{lab}} = 23.5^\circ$  and  $16.8^\circ$ , respectively, used in the  $(\alpha, \alpha'n)$  experiment are shown. The energy resolution is about 180 keV. The relative normalization between the two spectra is a factor of 3.4, corresponding to the different solid angles used in the coincidence experiment which roughly compensate the increase of the strength in the GR region at smaller angles.

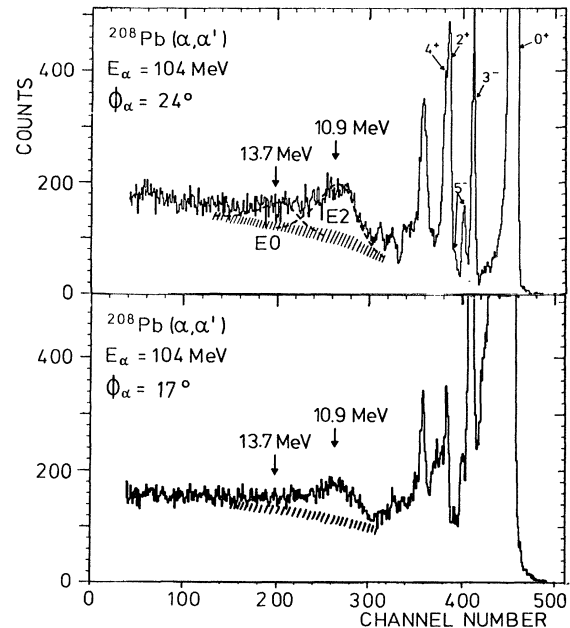


FIG. 5.  $\alpha$ -scattering spectra from  $^{208}\text{Pb}$  at  $E_\alpha = 104$  MeV at an excitation maximum (upper part) and minimum (lower part) of the giant quadrupole resonance.

Using a method, described in Ref. 6, which utilizes the time of flight of the  $\alpha$  particles as a second independent source of energy information, it could be proved that these spectra are practically free of experimental background. The prominent low lying states in  $^{208}\text{Pb}$  and the center of the  $E2$  GR ( $E_x \approx 10.9$  MeV) and of the  $E0$  GR ( $E_x \approx 13.7$  MeV) are labeled. The indicated background is of a physical nature, e.g., it is owing to nonresonant processes like quasifree scattering and multistep excitations. The resonant strength in the  $E0$  and  $E2$  regions in relation to the underlying background is obviously larger in the upper spectrum. One can estimate a ratio between resonant strength and the underlying continuum of roughly 1:1 in the center of the  $E2$  GR and of about 1:3 in the center of the  $E0$  GR for the spectrum measured in the cross section maximum. A quantitative analysis on the basis of DWBA calculations including all measured singles spectra and assuming pure  $E2$  and  $E0$  strength around 10.9 and 13.7 MeV, respectively, gives values of about 90%  $E2$  EWSR and 100%  $E0$  EWSR, which agree fairly well with the results of other groups.<sup>7,8</sup> These results, however, depend strongly on the assumed background, one of the main problems of GR experiments, discussed in more detail, e.g., in Ref. 1.

Our n-decay experiment<sup>5</sup> studying the  $E2$  GR region in  $^{208}\text{Pb}$  demonstrated that in the  $E2$  region, in addition, considerable strength of higher multiplicities is excited in  $\alpha$  scattering and that the  $E2$  EWSR strength has to be reduced to a value of about 50%. This can be seen immediately from Fig. 6, where the resonant strength decaying into the  $\frac{1}{2}^-$  and  $\frac{3}{2}^-$  states (predominantly  $E2$  strength) and the strength decaying into the  $\frac{13}{2}^+$  state (predominantly  $L \geq 4$  strength) are decomposed. From

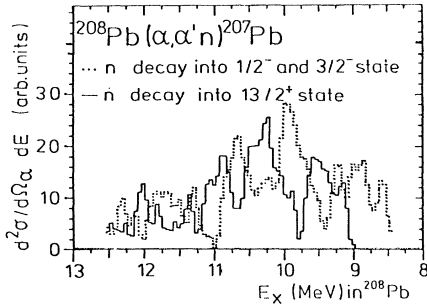


FIG. 6. Distribution of the resonant strength in the giant quadrupole resonance region of  $^{208}\text{Pb}$  from the neutron decay into the  $\frac{1}{2}^-$  and  $\frac{3}{2}^-$  states (dotted line) and into the  $\frac{13}{2}^+$  state (solid line).

this display it is obvious that not only the extracted  $E2$  sum rule exhaustion becomes lower, it also explains why in  $(\alpha, \alpha')$  singles spectra the  $E2$  GR usually appears as a relatively smooth bump. In our earlier  $(\alpha, \alpha')\gamma$  coincidence experiment<sup>4</sup> we found that also in the  $E0$  GR region noticeable strength of higher multiplicities ( $L > 0$ ) is excited in  $\alpha$  scattering. This result was recently confirmed by a detailed analysis of  $(\alpha, \alpha')$  small angle scattering.<sup>9</sup>

To give some impression of our on-line data, a typical time-of-flight spectrum of the neutrons in reference to the high frequency of the cyclotron is shown in the upper part of Fig. 7. The spectrum is taken threefold in order to simplify the control of the experiment. The neutrons from the target give broad bumps corresponding to their energy distribution. The prompt  $\gamma$  quanta from the target can be seen as narrow peaks in the spectrum with half widths of about 1.4 ns. From the measurements with monoenergetic

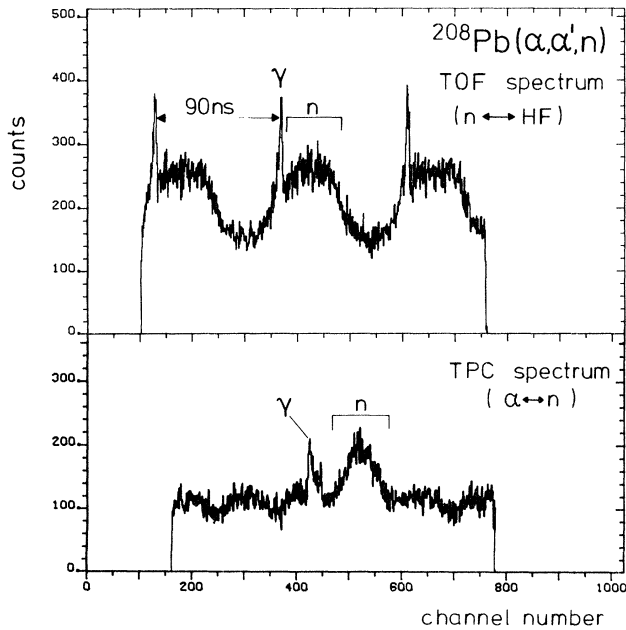


FIG. 7. Time-of-flight spectrum of the neutrons related to the high frequency of the cyclotron (upper part) and to the scattered  $\alpha$  particles (lower part).

neutrons at the Erlangen tandem accelerator mentioned earlier, this time resolution was found to be transferable directly to the neutrons in the energy region of interest. In the lower part of Fig. 7 a coincidence spectrum between an  $\alpha$  detector and a neutron detector is displayed showing the broad bump of the true  $\alpha$ -n coincidences together with the relatively small peak of  $\alpha$ - $\gamma$  coincidences. In order to obtain the spectra of the decay neutrons of the GR region in the various states of  $^{207}\text{Pb}$ , kinematical plots were made event by event. To get model independent branching ratios of the decay into the individual states as discussed for the decay of the  $E2$  region in Ref. 5 and the model independent strength distributions of the decay neutrons in the case where the decay into the individual states could no longer be resolved, we summed up the normalized spectra of the different angles of the n detectors after correcting for accidental coincidences. This averaging procedure is justified because the measured double differential cross section for a strength  $B$  (e.g., a GR) excited in  $\alpha$  scattering with subsequent n decay into states  $C$  of the residual nucleus can be written in the form

$$\frac{d^2\sigma}{d\Omega_\alpha d\Omega_n} = \frac{1}{4\pi} \frac{\Gamma_{nC}^B}{\Gamma^B} W(\theta_\alpha, \phi_\alpha; \theta_n, \phi_n) \frac{d\sigma}{d\Omega_\alpha}(\theta_\alpha, \phi_\alpha). \quad (1)$$

The angular correlation function factorizes into

$$W(\theta_\alpha, \phi_\alpha; \theta_n, \phi_n) = \sum_{KQ} \rho_{KQ}(J_B; \theta_\alpha, \phi_\alpha) \times F_K(J_B, J_C) C_{KQ}(\theta_n, \phi_n). \quad (2)$$

The statistical tensors  $\rho_{KQ}$  of the excited strength  $B$  with spin  $J_B$  depend on the excitation mechanism of the  $\alpha$ -scattering process. The  $F_K$  coefficients describe the n decay and contain combinations of the reduced transition matrix elements corresponding to the different possible angular momenta carried away by the neutrons. The  $C_{KQ}$  functions are renormalized spherical harmonics which give the dependence on the position of the n detector. The subscripts  $K$  and  $Q$  are limited by the spin  $J_B$  and the angular momenta transferred in the n decay. To get the branching ratios  $\Gamma_{nC}^B/\Gamma^B$  (and the n-decay spectrum for cases where the decay into the different states  $C$  can no longer be resolved) model independently, one has to measure the double differential cross section for a sufficient number  $N$  of special positions  $(\theta_{ni}, \phi_{ni})$  of the n detector out of the reaction plane. One then gets

$$\sum_{(\theta_{ni}, \phi_{ni})}^N W(\theta_\alpha, \phi_\alpha; \theta_{ni}, \phi_{ni}) = N \text{ average } W(\theta_\alpha, \phi_\alpha; \theta_n, \phi_n) = N, \quad (3)$$

and, with Eq. (1),

$$\frac{\Gamma_{nC}^B}{\Gamma^B} = \frac{\sum_{(\theta_{ni}, \phi_{ni})} \frac{d^2\sigma}{d\Omega_\alpha d\Omega_n}(\theta_\alpha, \phi_\alpha; \theta_{ni}, \phi_{ni})}{N \frac{d\sigma}{d\Omega_\alpha}(\theta_\alpha, \phi_\alpha)}. \quad (4)$$

The minimum number  $N$  for a complete average of the

angular correlation function depends on the value of  $J_B$  of the excited strength, in our case on the multipolarity of the GR of interest and that of the underlying background. The detector positions  $(\theta_{ni}, \phi_{ni})$  are fixed by the form of the spherical harmonics  $C_{KQ}(\theta_n, \phi_n)$ . For a pure monopole strength ( $J_B=0$ ) the angular correlation is isotropic ( $W=1$ ) and it is sufficient to measure at only one position ( $N=1$ ). In the case of quadrupole strength ( $J_B=2$ ) eight positions are needed. One set of angles  $(\theta_i, \phi_i)$  to fulfill Eq. (3) for this case is the set used in the present experiment.

Test calculations, where the excitation of strength of different multiplicities was calculated in DWBA, showed, however, that for the situation of the present experiment, the applied average of the angular correlation function  $W$  is also sufficient for higher multiplicities. For any  $J_B > 2$  and for the eight positions of our experiment, we found the maximum deviation of the average of  $W$  from the exact value of  $W$  to be less than 10%.

In the following we concentrate on the analysis of the decay of the  $E0$  GR region. Whereas quantitative extraction of a direct decay component was not possible from our experiments of Ref. 5, in the region of the  $E0$  GR a more precise and largely model independent extraction of the direct decay width is possible from the shape of the spectrum of the decay neutrons. In the case of a pure statistical decay, this spectrum should have an evaporation shape, which can be approximated by the well-known formula  $N(E_n) = E_n \exp(-E_n/T)$ , where  $E_n$  is the energy of the decay neutrons and  $T$  describes the nuclear temperature. An experimental excess of fast neutrons compared to this curve corresponding to the decay into the low lying hole states of the residual nucleus gives an estimate of the direct decay component. Applying this method in  $(\gamma, n)$  measurements to the decay of the  $E1$  GR in heavy nuclei, direct components of 5–15% have been extracted.<sup>10</sup> In a recent  $(\alpha, \alpha'n)$  coincidence experiment qualitative evidence for a direct decay component was also reported for the region of the  $E2$  GR in  $^{119}\text{Sn}$ .<sup>11</sup>

The discrimination between statistical and direct decay based on the shape of the decay spectrum, however, presumes that the number of states available in the residual nucleus is large enough so that besides the low lying one-hole states, a sufficient number of states with more complicated structure can be populated by the decay. This is not the case for the region of the  $E2$  GR ( $E_x \approx 10.5$  MeV) in  $^{208}\text{Pb}$  as discussed in Ref. 5, but it is sufficiently fulfilled for the region of the  $E0$  GR ( $E_x \approx 13.5$  MeV) studied in this work.

In Fig. 8 coincident spectra of the decay neutrons from the center of the  $E0$  GR ( $13 \text{ MeV} \leq E_x \leq 14 \text{ MeV}$ ) are shown for the measured maximum (upper part) and minimum (middle part) of the angular distribution of the resonant strength. These spectra, which are plotted as a function of the excitation energy in  $^{207}\text{Pb}$ , are normalized to the same total strength excited in  $^{208}\text{Pb}$  and summed over the different angles of the decay neutrons. The dashed line represents the evaporation curve of a pure statistical decay, which is adjusted simultaneously to the two spectra at small  $n$  energies (corresponding to excitation energies in  $^{207}\text{Pb}$  between about 3.0 and 4.5 MeV). The

respective nuclear temperature of  $T=0.7$  MeV (Ref. 12) agrees fairly well with statistical model predictions (compare, e.g., Ref. 13). The spectrum for the maximum (upper part) shows a clear excess of fast neutrons (hatched area), which has to be associated with a direct decay into the low lying hole states of  $^{207}\text{Pb}$ . The evaluation of this spectrum yields a value of about  $(5 \pm 1)\%$  for the excess concentrated in bump (a) and of about  $(3 \pm 1)\%$  for the excess in bump (b). Exploiting only this information, one extracts a direct decay component of  $(8 \pm 2)\%$  for the center of the  $E0$  GR. This value is related to the total strength, including the nonresonant background. An estimate for the direct decay component of the resonant strength alone can be obtained from the comparison of the maximum spectrum with the minimum spectrum (middle part of Fig. 8) and with a spectrum outside the resonance. The minimum spectrum (middle part) shows a considerably smaller excess of fast neutrons ( $2.5 \pm 1\%$ ) than the maximum spectrum. Therefore, we conclude that the excess of fast neutrons predominantly belongs to the decay of the resonant strength, the portion of which is larger in the maximum of the  $E0(E2)$  angular distribution. The different shape of the excess in both spectra will be discussed later.

In the lower part of Fig. 8 a decay spectrum corresponding to the excitation energies  $15 \text{ MeV} \leq E_x \leq 16 \text{ MeV}$  is shown for the maximum position of the  $\alpha$ -particle detectors.<sup>14</sup> It is obvious that the fraction of fast neutrons

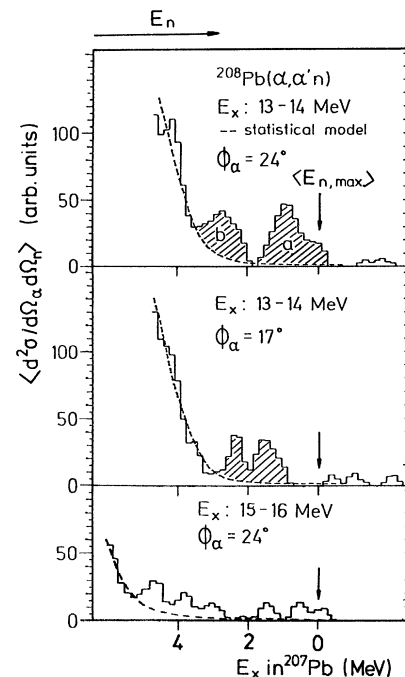


FIG. 8. Neutron decay spectra of the reaction  $^{208}\text{Pb}(\alpha, \alpha'n)^{207}\text{Pb}$  between 13 and 14 MeV excitation energy in  $^{208}\text{Pb}$  for the measured excitation maximum at  $24^\circ$  (upper part) and minimum at  $17^\circ$  (middle part) of the  $E0$  resonant strength, and between 15 and 16 MeV at  $24^\circ$  (lower part).

associated with a direct decay also in this spectrum, which again is normalized to the same total excited strength as the upper and middle spectra, is much smaller ( $2 \pm 1$ )% than for the maximum spectrum of the excitation energy region  $13 \text{ MeV} \leq E_x \leq 14 \text{ MeV}$ . This confirms the result that the direct decay component is much larger for the resonant strength than for the nonresonant background, which is not very surprising, because a large part of the nonresonant strength is excited in complicated multistep processes.

An upper limit for the direct decay component of the resonant strength can be deduced assuming a pure statistical decay of the background. With the resonance to background ratio of 1:3 from Fig. 5, one thus obtains from the excess of  $(8 \pm 2)\%$  extracted from the maximum spectrum a direct decay component of the resonant strength of about 20–25% as an upper limit. Taking the value of 2% from the lower spectrum of Fig. 8 as the direct decay component of the background, one ends up with the more realistic value of about 15–20% for the direct decay component of the resonant strength.

Some more details about the decay of the  $E0$  GR region into the low lying states of  $^{207}\text{Pb}$  can be deduced from Fig. 9, where the interesting section of the two upper spectra of Fig. 8 is plotted enlarged together with the level scheme of  $^{207}\text{Pb}$  and a decomposition of the spectra into Gaussians with widths of 500 keV corresponding to the experimental resolution and positions known from the level scheme. Owing to the relatively large statistical errors of the data (the smallest Gaussians drawn in the figure represent the limit of significance), one cannot extract quantitative information about the decay into the individual states. Nevertheless, one gets some remarkable qualitative results, which turn out to be absolutely stable in the fit. Obviously the shape of the strength distribution is different in both spectra. The spectrum referring to the maximum of the  $E0$  angular distribution ( $\phi_\alpha = 24^\circ$ ) shows a relatively

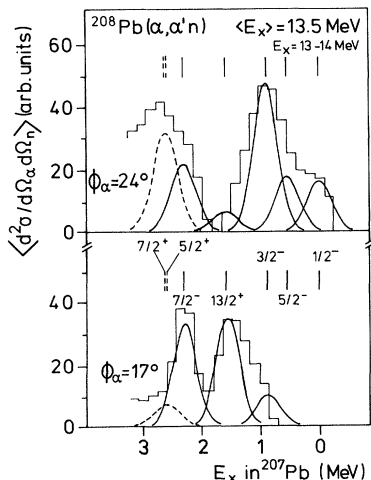


FIG. 9. Neutron decay from the center of the  $E0$  GR region in  $^{208}\text{Pb}$  into the low lying states of  $^{207}\text{Pb}$  for the measured excitation maximum (upper part) and minimum (lower part), together with a fit to the experimental data.

strong population of the three lowest states, the one-hole states with spins  $\frac{1}{2}^-$ ,  $\frac{5}{2}^-$ , and  $\frac{3}{2}^-$ , whereas the  $\frac{13}{2}^+$  “high spin” one-hole state is hardly populated. In the spectrum of the measured minimum the situation is the reverse. The  $\frac{7}{2}^-$  one-hole state is populated in both spectra with comparable intensity. This behavior can be explained using the angular momentum matching arguments discussed in detail in Ref. 5 for the  $E2$  GR region, which qualitatively also hold for the  $E0$  GR region. Transmission coefficients calculated for the discussed  $E0$  GR region in  $^{208}\text{Pb}$  show that the decay of  $E0$  and  $E2$  strength into the  $\frac{13}{2}^+$  state is strongly suppressed ( $< 5\%$  of the decay into the five lowest states in  $^{207}\text{Pb}$ ), that it is preferred for strength with higher multiplicities (especially  $L=6$ ), and that the  $\frac{7}{2}^-$  state with an “intermediate” spin is populated from  $E0$  and  $E2$  strength, as well as from strength with higher multiplicities. This result is valid also for the direct decay mode, as can be demonstrated by test calculations, which take into account the overlap between the  $ph$  wave functions of the resonant strength (taken from Refs. 15 and 16) and the different hole states. Therefore, we associate the much stronger population of the three “low spin” states in the maximum spectrum ( $\phi_\alpha = 24^\circ$ ) predominantly with the decay of the resonant  $E0$  and  $E2$  strength.

The relative strong population of the  $\frac{13}{2}^+$  state in the  $17^\circ$  spectrum, which is not seen in the  $24^\circ$  spectrum, shows that also in the region of the  $E0$  GR in  $^{208}\text{Pb}$  considerable strength of higher multiplicities is excited, especially  $E6$  strength, which has a maximum in the angular distribution at  $\phi_\alpha = 17^\circ$ , as can be seen from DWBA calculations. The presence of higher multipole strength in the  $E0$  GR region is confirmed in recent  $(\alpha, \alpha')$ -singles experiments.<sup>9,17</sup>

From the fit shown in Fig. 9 it is evident that the excess in the excitation region between about 2 and 3 MeV in  $^{207}\text{Pb}$ , especially in the upper spectrum, cannot be attached completely to the decay into the  $\frac{7}{2}^-$  state. As known from pickup reactions<sup>18</sup> in this region, no additional one-hole state, which should be populated preferably in a direct decay, is situated. On the other hand, from the four additional states in this energy region the  $\frac{5}{2}^+ - \frac{7}{2}^+$  doublet at  $E_x \approx 2.65 \text{ MeV}$ , drawn as dashed lines in the level scheme and included as one state in the fit, is known<sup>19</sup> as a pair of 1p-2h phonon-hole states, which arise from the coupling of the  $\frac{1}{2}^-$  ground state of  $^{207}\text{Pb}$  to the lowest  $3^-$  vibrational state in  $^{208}\text{Pb}$  at 2.61 MeV. Phonon-hole states should be populated preferably from such 2p-2h states in  $^{208}\text{Pb}$ , in which the 1p-1h doorway state of the GR is coupled to low lying phonon states in  $^{208}\text{Pb}$ . Within this interpretation a part of the enhancement in this region has to be added to the spreading width as a “preequilibrium component,” and the discussed value of 15–20% of the direct decay component has to be reduced to 12–18%.

In summary, the decay of the resonant isoscalar electric  $E0$  and  $E2$  GR's in the observed energy region of  $^{208}\text{Pb}$  contains, beside a dominant statistical component, also a small but significant ( $\approx 15\%$ ) direct contribution. This means that their decay properties are very similar to

those<sup>20</sup> of the isovector  $E1$  GR in  $^{208}\text{Pb}$ , and confirms the trend known from the decay of the  $E2$  GR in light and medium nuclei. In addition, considerable strength of multipolarities  $L \geq 4$  is found in the  $E0$  GR region of  $^{208}\text{Pb}$ . Moreover, this work gives evidence for a preequilibrium decay from special  $2p$ - $2h$  configurations of the GR's in  $^{208}\text{Pb}$  into one-phonon-one-hole states of  $^{207}\text{Pb}$ . The occurrence of such a preequilibrium decay mode, which of course needs further experimental proof, is of fundamen-

tal interest for the understanding of the decay paths of the GR's.<sup>21</sup>

#### ACKNOWLEDGMENTS

We would like to thank the staff of the Karlsruhe cyclotron for their cooperation. This work was supported by the Deutsche Forschungsgemeinschaft and by the Kernforschungszentrum Karlsruhe.

- 
- <sup>1</sup>J. Speth and A. van der Woude, Rep. Prog. Phys. **44**, 719 (1981).
- <sup>2</sup>K. T. Knöpfle, G. J. Wagner, P. Paul, H. Breuer, C. Mayer-Böricke, M. Rogge, and P. Turek, Phys. Lett. **74B**, 191 (1978).
- <sup>3</sup>K. T. Knöpfle, H. Riedesel, K. Schindler, G. J. Wagner, C. Mayer-Böricke, W. Oelert, M. Rogge, and P. Turek, *Lecture Notes in Physics* **92**, edited by B. A. Robson (Springer, Berlin, 1979), p. 944, and references given therein.
- <sup>4</sup>W. Eyrich, A. Hofmann, U. Scheib, S. Schneider, F. Vogler, and H. Rebel, Phys. Rev. Lett. **43**, 1369 (1979).
- <sup>5</sup>H. Steuer, W. Eyrich, A. Hofmann, H. Ortner, U. Scheib, R. Stamminger, D. Steuer, and H. Rebel, Phys. Rev. Lett. **47**, 1702 (1981).
- <sup>6</sup>W. Eyrich, H. Hassold, A. Hofmann, B. Mühldorfer, U. Scheib, and H. Rebel, Phys. Rev. C **24**, 2720 (1981).
- <sup>7</sup>M. N. Harakeh, K. van der Borg, T. Ishimatsu, H. P. Morsch, A. van der Woude, and F. E. Bertrand, Phys. Rev. Lett. **38**, 676 (1977).
- <sup>8</sup>D. H. Youngblood, C. M. Rozsa, J. M. Moss, D. R. Brown, and J. D. Bronson, Phys. Rev. Lett. **39**, 1188 (1977).
- <sup>9</sup>H. P. Morsch, P. Decowski, M. Rogge, P. Turek, L. Zemto, S. A. Martin, G. P. A. Berg, W. Hürlimann, J. Meissburger, and J. G. M. Römer, Phys. Rev. C **28**, 1947 (1983).
- <sup>10</sup>L. M. Young, Ph.D. thesis, University of Illinois, 1972.
- <sup>11</sup>K. Okada, H. Ejiri, T. Shibata, Y. Nagai, T. Motobayashi, H. Ohsumi, M. Nonmachi, A. Shimizu, and K. Maeda, Phys. Rev. Lett. **48**, 1382 (1982).
- <sup>12</sup>Although owing to the experimental threshold,  $n$  energies of  $E_n < 1.5$  MeV could not be taken into consideration for the fit, the value of  $T=0.7$  MeV is fixed within about 15%. This uncertainty is included in the errors of the values for the non-statistical decay components obtained from the analyses.
- <sup>13</sup>E. Vogt, Adv. Nucl. Phys. **1**, 261 (1968).
- <sup>14</sup>The comparison with spectra from the low energy side of the  $E0$  GR region is not convenient because there is the domain of the  $E2$  GR, the decay of which has been discussed already in Ref. 5.
- <sup>15</sup>G. A. Rinker and J. Speth, Nucl. Phys. **A306**, 360 (1978); and private communication.
- <sup>16</sup>E. Grecksch, W. Knüpfer, and M. G. Huber, Lett. Nuovo Cimento **14**, 505 (1975); and private communication.
- <sup>17</sup>T. Yamagata, S. Kishimoto, K. Yuasa, B. Saeki, K. Iwamoto, M. Tanaka, T. Fukuda, I. Miura, M. Inoue, and H. Ogata, Nucl. Phys. **A381**, 277 (1982).
- <sup>18</sup>S. Gales, G. M. Crawley, D. Weber, and B. Zwiigliniski, Phys. Rev. C **18**, 2475 (1978).
- <sup>19</sup>O. Häusser, F. C. Khanna, and D. Ward, Nucl. Phys. **A194**, 113 (1972).
- <sup>20</sup>J. R. Calarco, Ph.D. thesis, University of Illinois, 1969.
- <sup>21</sup>R. A. Broglia and P. F. Bortignon, Phys. Lett. **101B**, 135 (1981); *Proceedings of the Giant Multipole Resonances Topical Conference. Oak Ridge, 1980*, edited by F. E. Bertrand (Harwood, New York, 1980), p. 317.